Journal of Vibration Engineering & Technologies
https://doi.org/10.1007/s42417-024-01464-3

ORIGINAL PAPER

Fuzzy Logic Enhanced Second-Order Sliding Mode Controller Design for an Experimental Twin Rotor System Under External Disturbances

Hasan Omur Ozer[1] · **Yuksel Hacioglu**[2] · **Nurkan Yagiz**[2]

Received: 31 October 2023 / Revised: 22 May 2024 / Accepted: 7 June 2024
© The Author(s) 2024

Abstract

Background The twin rotor model is frequently studied by researchers because although it has a basic structure the coupled pitch and yaw motions are adequately represented. However, it is quite difficult to obtain an efficient controller due to external disturbances. Classical sliding mode controller (SMC), which is of first order, is recognized to be robust in case of parameter changes and external disturbances especially when the sliding motion takes place, but it possesses chattering in the control input which may damage the mechanical parts of the system.

Purpose In this study it was aimed to design a robust controller without chattering effect which will be used for the control of the twin rotor system in real time experiments.

Methods To remedy the chattering issue, a novel fuzzy logic enhanced second-order sliding mode controller (FSOSMC) based on super twisting algorithm is proposed. This controller suppresses chattering while enhancing the robustness of the controller where the sliding surface slope parameter is updated online via a fuzzy logic unit. Then the proposed controller is implemented on an experimental twin-rotor system which has highly nonlinear and coupled dynamics.

Results Real time experiments were performed on the twin rotor system using the proposed FSOSMC. For comparison purpose the SMC and second-order sliding mode controller (SOSMC) were also applied to the same system. The results have shown that the proposed controller increased the tracking performance without increasing the control effort while reducing the chattering.

Conclusions The experimental results verified the success of the designed FSOSMC, therefore it may be recommended for the robust and precise control of aerial vehicles.

✉ Hasan Omur Ozer
hasanomur.ozer@iuc.edu.tr

Yuksel Hacioglu
yukselh@iuc.edu.tr

Nurkan Yagiz
nurkany@iuc.edu.tr

[1] Department of Electricity and Energy, Vocational School of Technical Science, Istanbul University-Cerrahpaşa, Istanbul, Türkiye

[2] Department of Mechanical Engineering, Faculty of Engineering, Istanbul University-Cerrahpaşa, Istanbul, Türkiye

Published online: 01 July 2024

Graphical Abstract

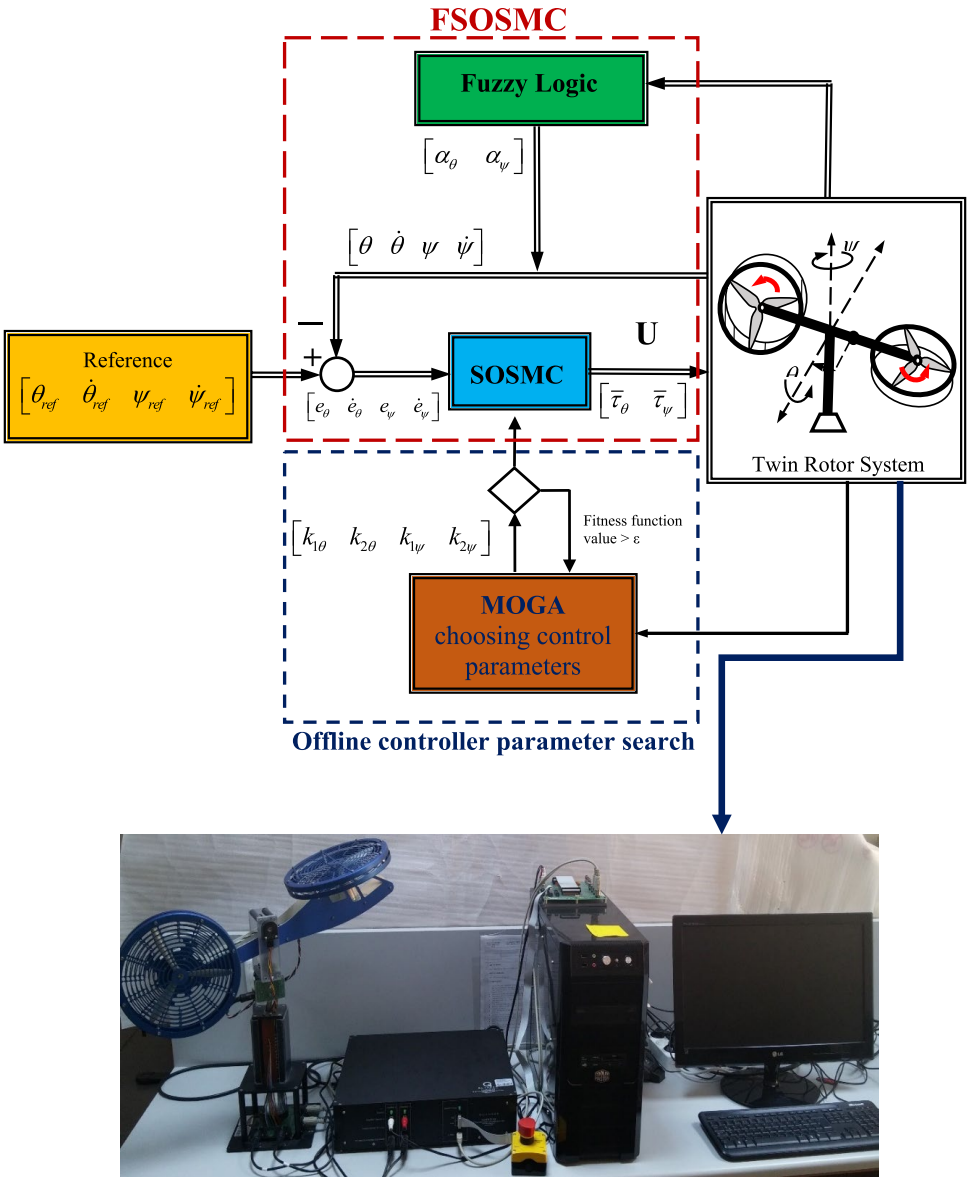

Keywords Fuzzy second order sliding mode control · Twin rotor model · Experimental results · Multi-objective genetic algorithm

Introduction

During the last decade, studies concerning twin rotor system have increased. It is a basic helicopter model used to study the hovering dynamics. This popularity stems from the similarity between those systems [1]. Tao et al. [2] controlled the twin rotor with fuzzy linear quadratic regulator (LQR). Taskin [3] investigated the performance of twin rotor system under hovering conditions with fuzzy logic controller (FLC). A hybrid proportional-integral-derivative (PID) controller was implemented to a twin rotor by Juang et. al. [4]. Aras and Kaynak [5] designed an interval type-2 fuzzy neural controller for the twin rotor system. The designed controller was compared with a traditional neuro-fuzzy structure and an interval type-2 fuzzy neural system. Hacioglu [6] proposed a new fuzzy logic algorithm to control angular motions of a twin rotor setup. The controller performance was verified via experiments. The control problem of highly nonlinear systems with varying operating conditions was investigated by Omar et al. [7]. They proposed an adaptive

neuro-fuzzy inference system (ANFIS) for a twin-rotor system. Juang et al. [8] designed a fuzzy PID control structure with a genetic algorithm for a regulation problem of twin rotor. Khakshour and Khanesar [9] proposed an adaptive learning algorithm for an interval type-2 fuzzy fractional order controller and applied it to a twin-rotor system. Mondal and Mahanta [10] designed an adaptive second-order sliding mode controller for a laboratory twin-rotor setup. The simulation findings of the controller showed sufficient tracking performance and robustness to external disturbances. A new sliding surface was proposed to handle cross-coupling affects in a twin rotor system by Ahmed et al. The sliding mode controller performance was improved with that surface [11]. Corradini et al. [12] investigated the stabilization problem for discrete-time linear controllable systems subject to actuator saturation with application to a twin-rotor system. In [13] sliding mode and backstepping controllers were designed and their performances were validated on a twin-rotor system via simulations. Raghavan and Thomas [14] presented an implementable model predictive controller for a twin rotor. Palepogu and Mahapatra [15] designed a sliding mode controller with state-varying gains for the control of yaw orientation of the twin rotor system. Zeghlache et al. [16] synthesized an adaptive fuzzy controller for the twin rotor system and verified it by experiments.

Classical sliding mode control (SMC) has a robust character [17, 18] and it is applicable to nonlinear as well as uncertain systems [19]. SMC was used in many applications like vehicle suspension control [20–22], seismic vibration control [23–25], robotics [26, 27] an so on. Insensitivity of the controlled system to external disturbances and parameter changes [28] is achieved when the system states are on the sliding surface. However, in practice, systems with sliding mode may face with chattering in control signal and this may damage the system's mechanical parts. There are a few techniques in literature to remedy this issue, that replaced the signum function with saturation [29] and sigmoid-like functions [30] as continuous approximations. However, as a result ideal sliding motion no more takes place. Hence, high order SMC technique was recommended by researchers to suppress or eliminate chattering [31, 32]. Particularly, Levant [32] presented a SOSM algorithm known as Super Twisting Algorithm (STA) and then it was used for control applications [32–37]. Rashad et al. [38] proposed an integral sliding mode controller for a twin-rotor system where the controller was augmented by a sliding mode disturbance observer to eliminate the discontinuity in the control signal. Tapia et al. [39] designed a sliding mode controller by using exact convex expressions for non-linear sliding surface and system. Finally, that method led to linear matrix inequalities that may be solved with convex optimization methods. A high-order sliding mode controller was proposed to control an active suspension model by Ozer et al. [40]. The simulations and experimental results of that controller showed sufficient ride comfort improvement while eliminating chattering.

The objective of this research is to design a robust controller without chattering effect which will be used for the control of the twin rotor system in real time experiments. In order to reach this aim we proposed a novel fuzzy logic enhanced second-order sliding mode controller. The controller is based on classical SOSMC with STA, but proposed controller is different from that since the slope parameter of the sliding surface is updated online via a fuzzy logic unit, which results in increased performance and robustness. Additionally, in order to eliminate ne need for exact mathematical model of the system, the designed controller utilizes an estimator for equivalent component of control input which is not the case in classical SOSMC available in literature. Then the performance of the proposed controller was confirmed by real time experiments on a twin rotor system which has highly nonlinear dynamics. To compare the success of the proposed controller, a classical SMC (first order) and a classical SOSMC are also applied to the experimental twin rotor system. The results have shown that the proposed controller increased the tracking performance without increasing the control effort while reducing the chattering.

Controller Design

In this section first, the twin rotor model is presented and then the proposed FSOSMC is designed.

Twin Rotor Model

The twin rotor model is often studied by engineers and academicians because it possesses a basic structure but still cross coupled pitch and yaw motions are adequately represented. Figure 1 presents the physical model. Here, m_{hel} stands for the total mass of the helicopter, distance from the mass center to the pitch axis along the helicopter body is denoted with l, B_{pitch} and B_{yaw} are the viscous damping for pitch and yaw motions, I_{pitch} and I_{yaw} are the moment of inertia for pitch and yaw motions. Here, θ and ψ are angular displacements for the pitch and yaw motions and $\overline{\tau_\theta}, \overline{\tau_\psi}$ stand for the actuator moments. Parameters of the model are given in Table 5 in "Appendix 1".

The mathematical model for the twin rotor system was obtained using Lagrange's equations. In order to make the text self-contained without disrupting its flow, the energy functions required for the Lagrange's method are presented in "Appendix 1". The equations of motion are:

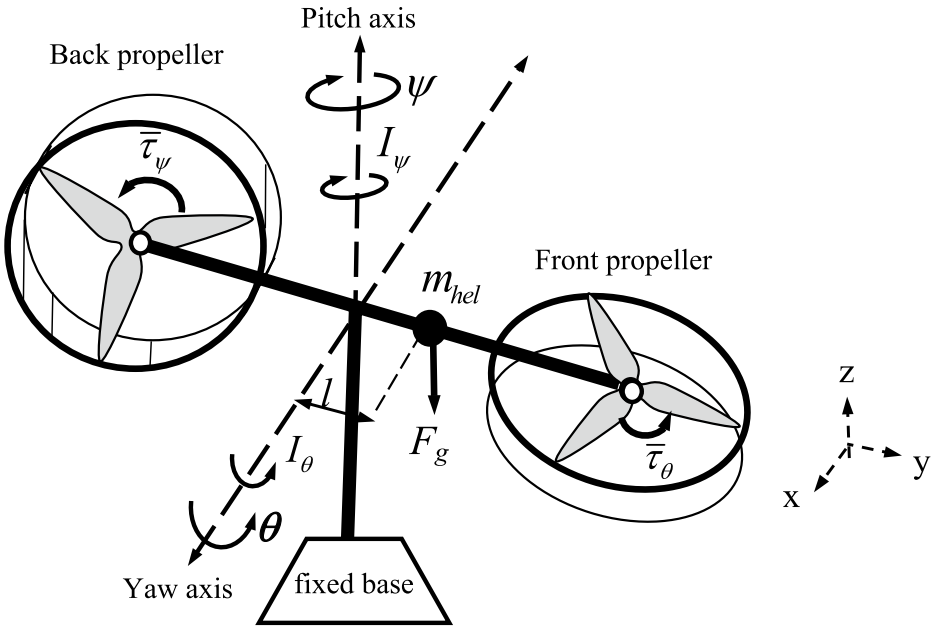

Fig. 1 Physical model of the twin rotor

$$m_{hel}l^2\ddot{\theta} + I_{pitch}\ddot{\theta} + m_{hel}l^2(\dot{\psi})^2\cos(\theta)\sin(\theta) + B_{pitch}\dot{\theta} + m_{hel}glcos(\theta) = \overline{\tau_\theta} + \widetilde{d_\theta} \tag{1}$$

$$m_{hel}l^2\ddot{\psi}cos^2(\theta) - 2m_{hel}l^2\dot{\theta}(\dot{\psi})\cos(\theta)\sin(\theta) + I_{yaw}\ddot{\psi} + B_{yaw}\dot{\psi} = \overline{\tau_\psi} + \widetilde{d_\psi} \tag{2}$$

Here $\widetilde{d_\theta}$ and $\widetilde{d_\psi}$ denote the external disturbances. State variables are chosen as:

$$\begin{bmatrix} x_1 & x_2 & x_3 & x_4 \end{bmatrix}^T = \begin{bmatrix} \theta & \dot{\theta} & \psi & (\dot{\psi}) \end{bmatrix}^T \tag{3}$$

Then twin rotor state equations are:

$$\dot{x_1} = x_2 \tag{4}$$

$$\dot{x_2} = \frac{-m_{hel}l^2(x_4)^2\cos(x_1)\sin(x_1) - B_{pitch}x_2 - m_{hel}glcos(x_1)}{(m_{hel}l^2 + I_{pitch})} + \frac{\overline{\tau_\theta}}{(m_{hel}l^2 + I_{pitch})} + \overline{d_\theta} \tag{5}$$

$$\dot{x_3} = x_4 \tag{6}$$

$$\dot{x_4} = \frac{2m_{hel}l^2(x_2)(x_4)\cos(x_1)\sin(x_1) - B_{yaw}(x_4)}{m_{hel}l^2cos^2(x_1) + I_{yaw}} + \frac{\overline{\tau_\psi}}{m_{hel}l^2cos^2(x_1) + I_{yaw}} + \overline{d_\psi} \tag{7}$$

The Proposed Fuzzy Second Order Sliding Mode Controller (FSOSMC)

A new fuzzy second-order SMC depending on super twisting algorithm is given in present section which uses an estimator for equivalent control. In literature, second-order sliding mode was defined by Levant [32, 34] as the motion on non-empty set $\sigma = \dot{\sigma} = 0$ which consists of locally Filippov trajectories where $\sigma = \dot{\sigma}$ are assumed to be continuous. Consider that equations of the system are given as:

$$\dot{\eta_1} = \eta_2 \tag{8}$$

$$\dot{\eta_2} = f(\eta_1, \eta_2) + g(\eta_1, \eta_2)\overline{u} + \overline{d} \tag{9}$$

where η_1 and η_2 are state variables, $\overline{u}$ is the control input, $\overline{d}$ stand for exogenous disturbance. $g(\eta_1, \eta_2)$ and $f(\eta_1, \eta_2)$ are nonlinear functions of the state variables. The sliding surface is chosen as

$$\sigma = \alpha(\eta_{1r} - \eta_1) + (\dot{\eta}_{1r} - \dot{\eta}_1) \tag{10}$$

where the sliding surface parameter is $\alpha > 0$. By taking the time derivative of the Eq. (10) and using Eqs. (8) and (9)

$$\dot{\sigma} = \alpha(\eta_{2r} - \eta_2) + \dot{\eta}_{2r} - f(\eta_1, \eta_2) - g(\eta_1, \eta_2)\overline{u} - \overline{d} \tag{11}$$

Then by using following definitions

$$\phi(\eta_1, \eta_2) = \alpha(\eta_{2r} - \eta_2) + \dot{\eta}_{2r} - f(\eta_1, \eta_2) \tag{12}$$

$$u = -g(\eta_1, \eta_2)\bar{u} \tag{13}$$

$$d = -\bar{d} \tag{14}$$

then

$$\dot{\sigma} = \phi(\eta_1, \eta_2) + u + d \tag{15}$$

During the analysis it was presumed that exogenous disturbing effect d is limited as $|d| \le \Delta\sqrt{|\sigma|}$, $\Delta > 0$. Additionally, when $\dot{\sigma} = 0, d = 0$, then equivalent control is calculated to be:

$$u_{eq} = -\phi(\eta_1, \eta_2) \tag{16}$$

To design the discontinuous component u_{dc} of the control input, the super twisting algorithm suggested in [32] is utilized.

$$u_{dc} = -k_1|\sigma|^{1/2}sign(\sigma) + \upsilon \tag{17}$$

$$\dot{\upsilon} = -k_2 sign(\sigma) \tag{18}$$

Now the entire control law is,

$$u = u_{dc} + u_{eq} \tag{19}$$

Stability validation is carried out, via Lyapunov function candidate [41].

$$V = 2k_2|\sigma| + \frac{1}{2}\upsilon^2 + \frac{1}{2}\left(k_1|\sigma|^{1/2}sign(\sigma) - \upsilon\right)^2 \tag{20}$$

Let's arrange this function as

$$V = \xi^{\mathrm{T}}\mathbf{P}\xi \tag{21}$$

in this quadratic form

$$\xi^{\mathrm{T}} = \begin{bmatrix} |\sigma|^{1/2}sign(\sigma) & \upsilon \end{bmatrix} \tag{22}$$

$$\mathbf{P} = \begin{bmatrix} 2k_2 + \frac{{k_1}^2}{2} & \frac{-k_1}{2} \\ \frac{-k_1}{2} & 1 \end{bmatrix} \tag{23}$$

Taking the time derivative of Eq. (21)

$$\begin{aligned} \dot{V} &= \dot{\xi}^{\mathrm{T}}\mathbf{P}\xi + \xi^{\mathrm{T}}\mathbf{P}\dot{\xi} \\ &= \dot{\sigma}sign(\sigma)\left(2k_2 + \frac{1}{2}{k_1}^2\right) \\ &\quad - k_1\dot{\upsilon}|\sigma|^{1/2}sign(\sigma) - \frac{k_1\upsilon\dot{\sigma}}{2|\sigma|^{1/2}} + 2\dot{\upsilon}\upsilon \end{aligned} \tag{24}$$

By using Eqs. (15)–(19)

$$\begin{aligned} \dot{V} &= \left[-k_1|\sigma|^{1/2}sign(\sigma) + \upsilon + d\right]sign(\sigma)\left(2k_2 + \frac{1}{2}k_1^2\right) \\ &\quad - k_1\left[-k_2 sign(\sigma)\right]|\sigma|^{1/2}sign(\sigma) \\ &\quad - \frac{k_1\upsilon\left[-k_1|\sigma|^{1/2}sign(\sigma) + \upsilon + d\right]}{2|\sigma|^{1/2}} + 2\left[-k_2 sign(\sigma)\right]\upsilon \\ &= -\left(k_1k_2 + \frac{k_1^3}{2}\right)|\sigma|^{1/2} + k_1^2\upsilon sign(\sigma) - \frac{k_1\upsilon^2}{2|\sigma|^{\frac{1}{2}}} \\ &\quad - d(t,\sigma)\frac{k_1\upsilon}{2|\sigma|^{\frac{1}{2}}} + d(t,\sigma)\left[\left(2k_2 + \frac{1}{2}k_1^2\right)sign(\sigma)\right] \end{aligned} \tag{25}$$

For the last two terms on the right side of Eq. (25) by using $|d| \le \Delta\sqrt{|\sigma|}$ it is found that

$$-\frac{k_1\upsilon}{2}\frac{d(t,\sigma)}{|\sigma|^{\frac{1}{2}}} \le -\frac{k_1\upsilon}{2}\Delta sign(\sigma) \tag{26}$$

$$d(t,\sigma)\left(2k_2 + \frac{1}{2}{k_1}^2\right)sign(\sigma) \le \Delta|\sigma|^{1/2}\left(2k_2 + \frac{1}{2}{k_1}^2\right) \tag{27}$$

After that Eq. (25) turns into

$$\begin{aligned} \dot{V} &\le -\left(k_1k_2 + \frac{{k_1}^3}{2}\right)|\sigma|^{1/2} + {k_1}^2\upsilon sign(\sigma) - \frac{k_1\upsilon^2}{2|\sigma|^{1/2}} \\ &\quad + \Delta\left(2k_2 + \frac{1}{2}{k_1}^2\right)|\sigma|^{1/2} - \frac{k_1\upsilon}{2}\Delta sign(\sigma) \end{aligned} \tag{28}$$

which may be written as

$$\dot{V} \le \frac{-k_1}{2|\sigma|^{1/2}}\xi^{\mathrm{T}}\mathbf{Q}\xi \tag{29}$$

where

$$\mathbf{Q} = \begin{bmatrix} 2k_2 + {k_1}^2 - \left(\frac{4k_2}{k_1} + k_1\right)\Delta & -k_1 + \frac{\Delta}{2} \\ -k_1 + \frac{\Delta}{2} & 1 \end{bmatrix} \tag{30}$$

Here, if k_1 and k_2 satisfy,

$$k_1 > 2\Delta \tag{31}$$

$$k_2 > \frac{k_1\Delta^2}{8(k_1 - 2\Delta)} \tag{32}$$

then, sliding surface is attained since $\dot{V} < 0$ is negative definite.

In practice, system parameters in $\phi(\eta_1, \eta_2)$ may be uncertain or unknown. Thus, the evaluated equivalent control signal may differ from the actual one. Thus, an estimation for equivalent control $\hat{u}_{eq}$ is utilized in this

research which is acquired by filtering entire control input with a low-pass filter [40]. Thereafter, estimated equivalent control becomes:

$$\hat{u}_{eq} = \frac{\varepsilon}{s+\varepsilon} u \tag{33}$$

Here ε is cut-off frequency. With this estimation this controller is different from existing second order sliding mode controllers in literature. It is assumed that low frequency component of the control input characterizes the signal and high frequency part presents unmodeled dynamics. Here, if ε is properly adjusted the output of the filter will well represent equivalent control [18], and system's stability is maintained. Then entire control input of the designed SOSMC is

$$\overline{u} = -g^{-1}(\eta_1, \eta_2) u \tag{34}$$

$$u = \hat{u}_{eq} - k_1 |\sigma|^{1/2} sign(\sigma) + \upsilon \tag{35}$$

$$\dot{\upsilon} = -k_2 sign(\sigma) \tag{36}$$

$$\dot{\hat{u}}_{eq} = \varepsilon (u - \hat{u}_{eq}) \tag{37}$$

Genetic Algorithm (GA) is an optimization method that motivated by natural selection principles. GA that work according to the probability rules require only the objective function. This method has searched a specific part of the solution space. Thus, complex problems have been solved effectively. The GA can benefit from better solutions with respect to different objectives to create new nondominated solutions of the Pareto front. Multi-objective genetic algorithm (MOGA) does not require most users to weigh targets and scaling [42].

In this study, gain of the controllers will be searched using fitness functions $\beta_i (i = 1,2, \ldots, 10)$ given below. It is aimed to reduce tracking errors and suppress chattering.

$$\beta_1 = \sum_{i=1}^{n} \left| \theta_{refi} - \theta_i \right| \tag{38}$$

$$\beta_2 = \sum_{i=1}^{n} \left| \psi_{refi} - \psi_i \right| \tag{39}$$

$$\beta_3 = \frac{1}{\sqrt{n}} \left[\sum_{i=1}^{n} \left(\dot{u}_{\theta i} \right)^2 \right]^{1/2} \tag{40}$$

$$\beta_4 = \frac{1}{\sqrt{n}} \left[\sum_{i=1}^{n} \left(\dot{u}_{\psi i} \right)^2 \right]^{1/2} \tag{41}$$

$$\beta_5 = dimension \left[\ddot{\theta}_i \rightarrow \left\{ \begin{array}{lll} \ddot{\theta}_i < 0 & and & \ddot{\theta}_{i-1} > 0 \\ \ddot{\theta}_i > 0 & and & \ddot{\theta}_{i-1} < 0 \end{array} \right\} \right] \tag{42}$$

$$\beta_6 = dimension \left[\ddot{\psi}_i \rightarrow \left\{ \begin{array}{lll} \ddot{\psi}_i < 0 & and & \ddot{\psi}_{i-1} > 0 \\ \ddot{\psi}_i > 0 & and & \ddot{\psi}_{i-1} < 0 \end{array} \right\} \right] \tag{43}$$

$$\beta_7 = \frac{1}{n} \sum_{i=1}^{n} \left| u_{\theta i} - \frac{1}{n} \sum_{i=1}^{n} |u_{\theta i}| \right| \tag{44}$$

$$\beta_8 = \frac{1}{n} \sum_{i=1}^{n} \left| u_{\psi i} - \frac{1}{n} \sum_{i=1}^{n} |u_{\psi i}| \right| \tag{45}$$

$$\beta_9 = \frac{1}{n} \sum_{i=1}^{n} \left| \ddot{\theta}_i - \frac{1}{n} \sum_{i=1}^{n} |\ddot{\theta}_i| \right| \tag{46}$$

$$\beta_{10} = \frac{1}{n} \sum_{i=1}^{n} \left| \ddot{\psi}_i - \frac{1}{n} \sum_{i=1}^{n} |\ddot{\psi}_i| \right| \tag{47}$$

Here the functions β_1, β_2 account for the success of controller in trajectory tracking. The functions β_3, β_4 account for fluctuations in control input. For the acceleration signal the β_5, β_6 denote the number of crossing from zero. The fitness functions $\beta_7, \beta_8, \beta_9, \beta_{10}$, account for the mean values of amplitudes of the control input and angular acceleration. Then, for the gain parameters the optimum values obtained by MOGA for twin rotor system are presented in Table 1.

In this study, we also present a fuzzy logic methodology where, the parameters of sliding surface $(\alpha_\theta, \alpha_\psi)$ of SOSMC are changed by the fuzzy logic unit. Figure 2 depicts membership functions for all variables that are in triangular shape. Abbreviated labels were utilized to name the membership functions. For the input variables NB is negative big, NS is negative small, Z is zero, PS is positive small, and PB

Table 1 Gains of the controllers

SOSMC	$k_{1\theta}$	9.0
	$k_{2\theta}$	7.25
	$k_{1\psi}$	2.7
	$k_{2\psi}$	2.11
FSOSMC	$k_{1\theta}$	5.80
	$k_{2\theta}$	0.67
	$k_{1\psi}$	3.83
	$k_{2\psi}$	0.15

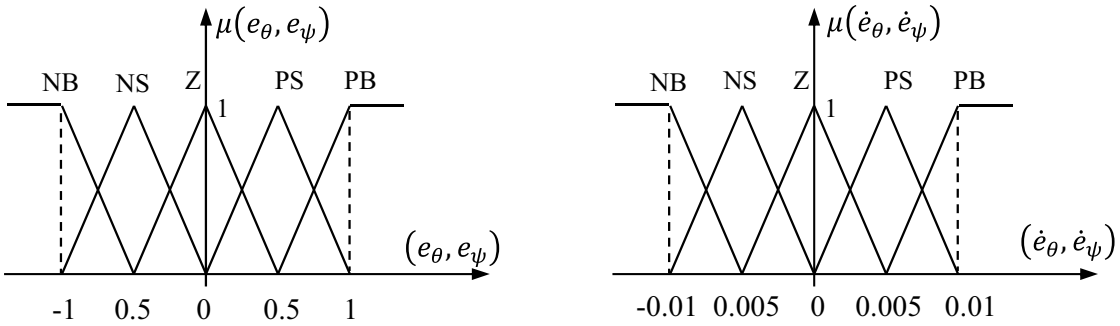

(a) Membership functions of error and derivative of error

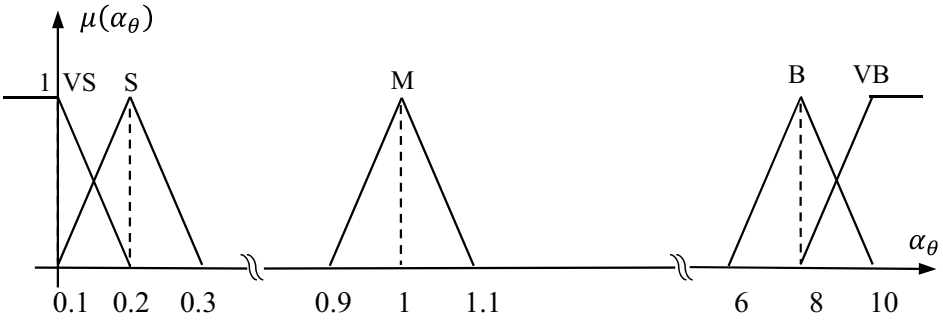

(b) Membership functions of α_θ

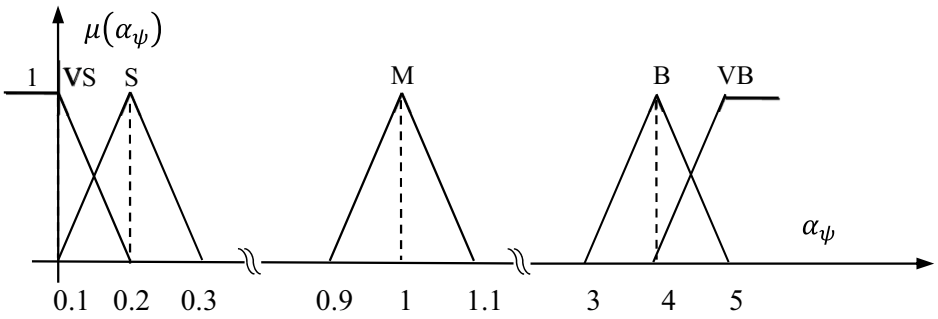

(c) Membership functions of α_ψ

Fig. 2 The membership functions of fuzzy logic

Table 2 Fuzzy rules

e \ $\dot{e}$	NB	NS	Z	PS	PB
NB	M	S	VS	S	M
NS	B	M	S	M	B
Z	VB	B	M	B	VB
PS	B	M	S	M	B
PB	M	S	VS	S	M

is positive big. For the output variables VS is very small, S is small, M is medium, B is big, and VB is very big.

The rules for the designed fuzzy logic unit are given in Table 2. The rule table is a adopted from [43]. Those decision rules were arranged in the IF–THEN form for the α_θ and α_ψ components.

$$\text{IF } e_\theta = NB \quad \text{and} \quad \text{IF } \dot{e}_\theta = Z \text{ THEN } \alpha_\theta = VS \tag{48}$$

$$\text{IF } e_\psi = Z \quad \text{and} \quad \text{IF } \dot{e}_\psi = PB \text{ THEN } \alpha_\psi = VB \tag{49}$$

If the rules are investigated, it observed that the manner behind is to rotate the sliding surface to force the system reach to the sliding surface faster. This will result in increased tracking performance and robustness for the designed FSOSMC. The overall structure of the proposed FSOSMC is presented in Fig. 3.

Experimental Setup and Results

Experimental Setup

Figure 4 shows the twin rotor experimental setup [44], which includes personal computer, data acquisition card and amplifier. Here the twin rotor system has two degrees of freedom. It is attached on a stationary base, and it has front and rear propellers, which are rotated via DC motors. The thrust force of the front and rear propellers cause motion about the pitch (horizontal axis) and yaw (vertical axis) axes. Two encoders were utilized to measure the pitch and yaw motions. The range of pitch motion (angle θ) is between -40.3 and 36 degrees. On the other hand, rotation about yaw axis is free thus the range of yaw motion (angle ψ) is 360 degrees. If $\theta = 0$, then the system is horizontal to the ground. Quanser

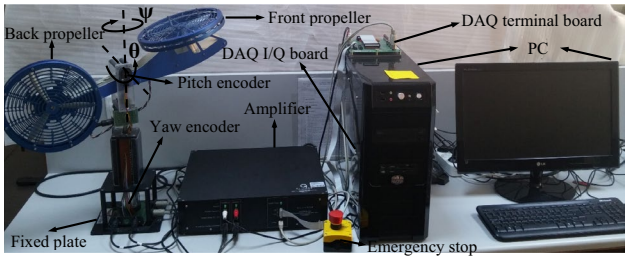

Fig. 4 The twin rotor model experimental setup

data acquisition card (DAQ) is utilized for data transmission. The voltage signals provided by the controller are transmitted to the amplifier which operates the direct current motors of the propellers. Control voltage limit is ± 24 V. For the real-time experiments the sampling period is set to 0.001 s. Parameters of the twin rotor system are given in Table 5 in "Appendix 1".

Control Laws for Experimental Setup

If governing state equations in Eqs. (4)–(7) are used, then control inputs of the suggested FSOSMC for twin rotor are obtained as

$$\overline{\tau_\theta} = -\left(m_{hel} l^2 + I_{pitch}\right)\tau_\theta \tag{50}$$

$$\tau_\theta = \hat{\tau}_{\theta eq} - k_{1\theta}\left|\alpha_\theta\left(x_{1r} - x_1\right) + \dot{x}_{1r} - x_2\right|^{\frac{1}{2}} sign\left(\alpha_\theta\left(x_{1r} - x_1\right) + \dot{x}_{1r} - x_2\right) + \upsilon_\theta \tag{51}$$

$$\dot{\upsilon_\theta} = -k_{2\theta}\left\{sign\left(\alpha_\theta\left(x_{1r} - x_1\right) + \dot{x}_{1r} - x_2\right)\right\} \tag{52}$$

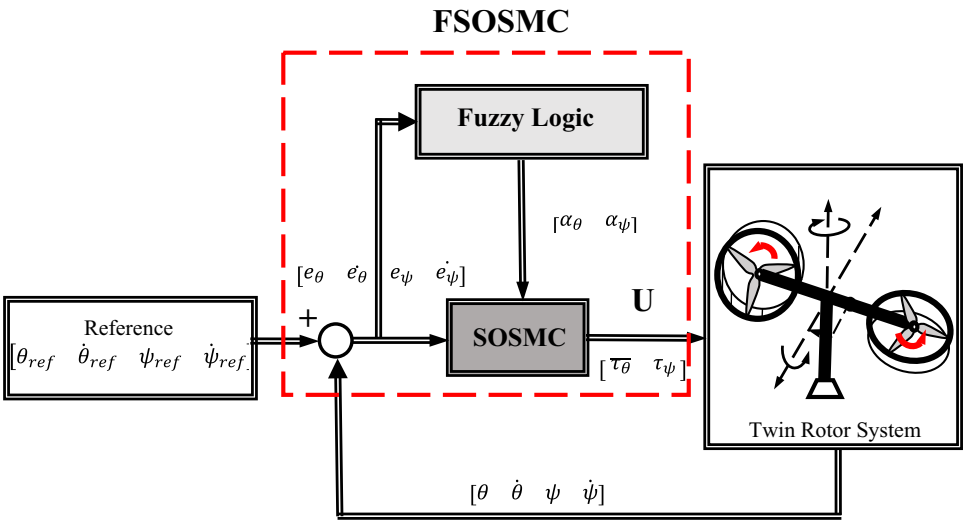

Fig. 3 Block diagram for the designed FSOSMC

$$\dot{\hat{\tau}}_{eq\theta} = \varepsilon\left(\tau_\theta - \hat{\tau}_{eq\theta}\right) \tag{53}$$

$$\overline{\tau_\psi} = -\left(m_{hel}l^2 cos^2(x_1) + I_{yaw}\right)\tau_\psi \tag{54}$$

$$\begin{aligned}\tau_\psi = \hat{\tau}_{\psi eq} - k_{1\psi}\left|\alpha_\psi\left(x_{3r} - x_3\right) + \dot{x}_{3r} - x_4\right|^{\frac{1}{2}} \\ sign\left(\alpha_\psi\left(x_{3r} - x_3\right) + \dot{x}_{3r} - x_4\right) + \upsilon_\psi\end{aligned} \tag{55}$$

$$\dot{\upsilon}_\psi = -k_{2\psi}\left\{sign\left(\alpha_\psi\left(x_{3r} - x_3\right) + \dot{x}_{3r} - x_4\right)\right\} \tag{56}$$

$$\dot{\hat{\tau}}_{eq\psi} = \varepsilon\left(\tau_\psi - \hat{\tau}_{eq\psi}\right) \tag{57}$$

$$\overline{\tau_\theta} = K_{pp}V_{mp} + K_{py}V_{my} \tag{58}$$

$$\overline{\tau_\psi} = K_{yp}V_{mp} + K_{yy}V_{my} \tag{59}$$

Equations (58) and (59) are simultaneously solved to obtain the control voltages as below:

$$V_{mp} = \frac{K_{py}\overline{\tau_\psi} - K_{yy}\overline{\tau_\theta}}{K_{py}K_{yp} - K_{pp}K_{yy}} \tag{60}$$

$$V_{my} = \frac{K_{pp}\overline{\tau_\psi} - K_{yp}\overline{\tau_\theta}}{K_{yy}K_{pp} - K_{py}K_{yp}} \tag{61}$$

In this study, the control signals are the torques and in the experimental system they are converted to voltage signals $\left(V_{mp}, V_{my}\right)$ as given in Eqs. (60)–(61). In the equations above $K_{yy}, K_{pp}, K_{py}, K_{yp}$ are the thrust force constants defined in "Appendix 1".

Performance Indexes

To measure the performance of the designed controllers following indexes are defined in this study.

Integral of time multiplied absolute error (ITAE) index [45, 46]:

$$ITAE = \int_0^t t|e|dt \tag{62}$$

Control effort index (CEI) [47]:

$$CEI = \frac{1}{\sqrt{n}}\left[\sum_{i=1}^{n}\left(u_i\right)^2\right]^{1/2} \tag{63}$$

Chattering index (CI) [47]:

$$CI = \frac{1}{\sqrt{n}}\left[\sum_{i=1}^{n}\left(\dot{u}_i\right)^2\right]^{1/2} \tag{64}$$

The first performance index (ITAE) presents the error value of the angular displacement on time vector and heavily penalizes the errors late in time. The second index (CEI) measures the control effort utilized by the control algorithm. The third index (CI) measures the chattering in the control input. The CEI and CI are the root mean square values of relevant signals.

Experimental Results

Experimental results for the twin rotor model using proposed FSOSMC are presented in this section. The experimental results with first order SMC and classical SOSMC with super twisting algorithm are also presented for comparison purpose. To make the article self-contained, the design of the classical first order SMC is presented in "Appendix 2" along with parameters in Table 6. The control laws for the classical SOSMC may be easily obtained from the Eqs. (50)–(57) without using equivalent control parts. That is only the discontinuous parts due to the super twisting algorithm are used and resulting control laws for the classical SOSMC are presented in "Appendix 2". Furthermore, the sliding surface parameters of pitch and yaw motions are obtained by fuzzy logic units for the FSOSMC. The variation of sliding surface parameters are presented in Fig. 5. It is seen that the controller dynamically changes the sliding surface parameter according to the error states of the system.

Time responses for the twin rotor system without external disturbance are presented in Fig. 6. It is observed from this figure that the reference trajectories for pitch and yaw

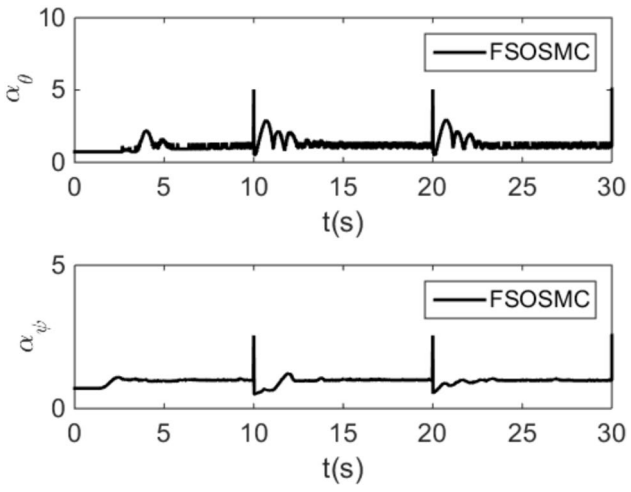

Fig. 5 Variation of the sliding surface parameters (without disturbance)

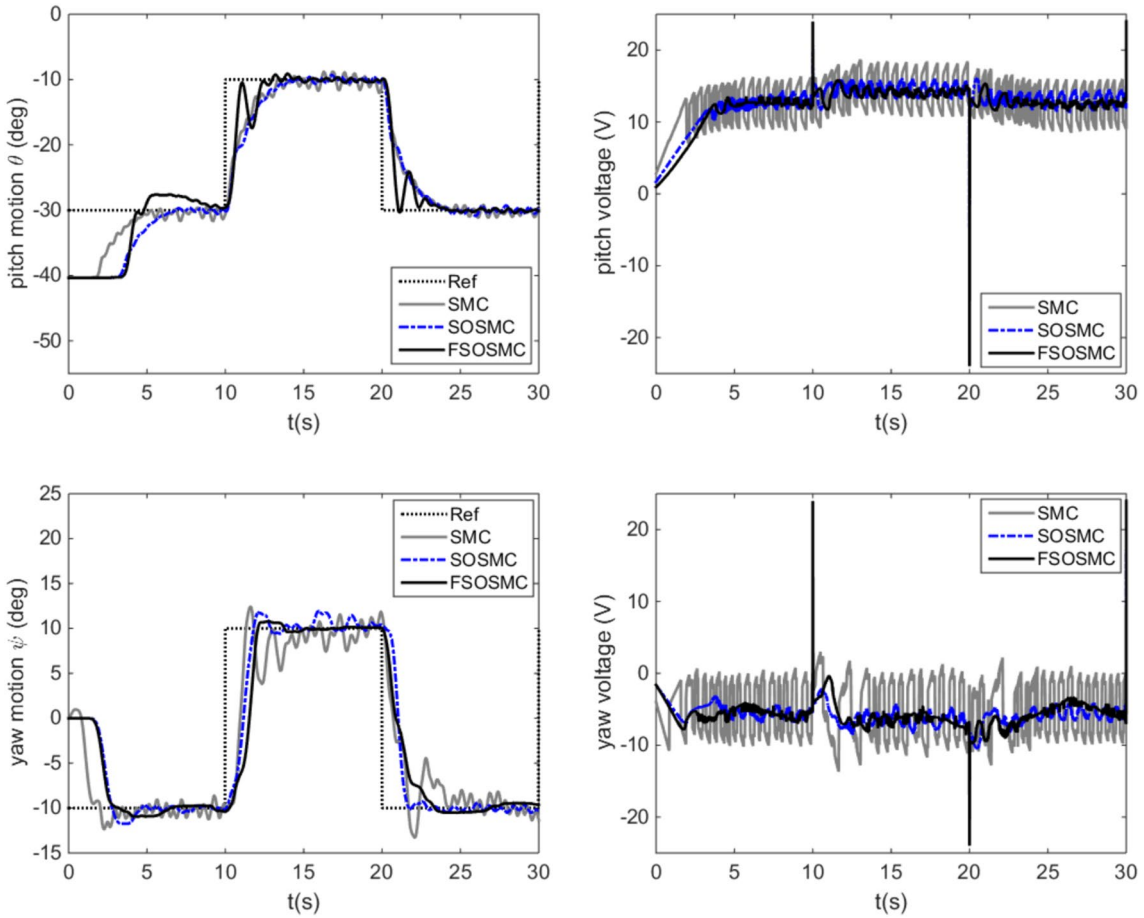

Fig. 6 Experimental results (without disturbance)

motion are successfully tracked by all controllers whereas the FSOSMC is most successful one since the oscillatory motions vanishes rapidly. This success is due to the online tuning of the sliding surface parameters by the fuzzy logic unit. Additionally, if the control inputs are investigated it reveals that chattering, that is high frequency fluctuations in control signal, arises in case of SMC. On the other hand, the classical SOSMC and FSOSMC cases are almost free of chattering.

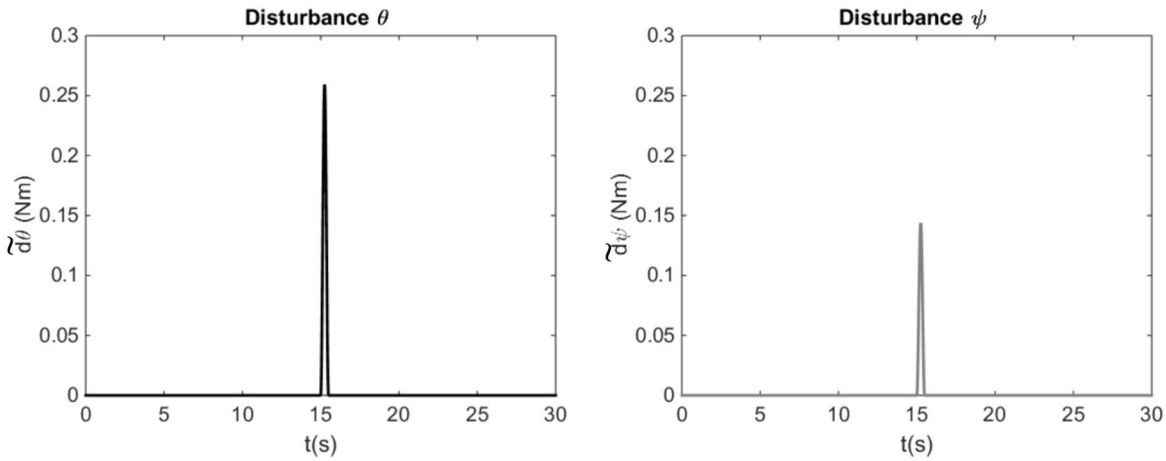

Fig. 7 Disturbances for pitch and yaw motions

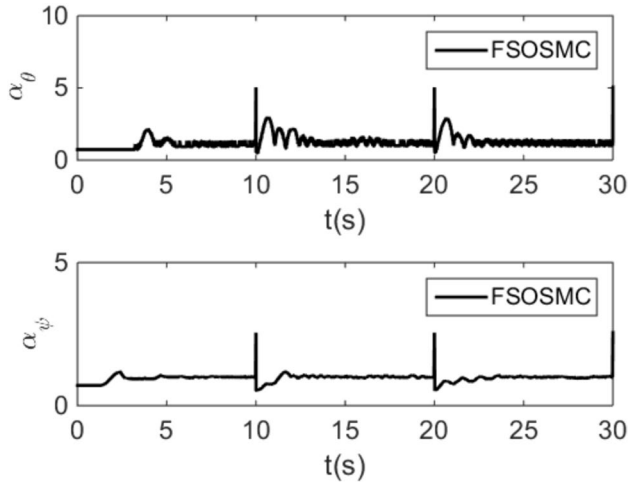

Fig. 8 Variation of the sliding surface parameters (with disturbance)

To compare the robustness performance of the controllers half sinusoidal exogenous disturbances were added to the control inputs. Frequency of the disturbances is 2 Hz and amplitude for $\widetilde{d_\theta}$ is 0.2592 Nm, and for $\widetilde{d_\psi}$ is 0.1437 Nm as given in Fig. 7.

Time responses for the twin rotor system under external disturbances are now presented. Figure 8 shows the variation of sliding surface parameters that are online tuned by the fuzzy logic unit. As seen from the figure they are dynamically changed according to the state of the system. Figure 9 depicts the time responses in case of external disturbance. It is observed from this figure that the magnitudes of angular displacements and control voltages were reduced via both classical SOSMC and proposed FSOSMC controller. Furthermore, it is worth noting that chattering

Fig. 9 Experimental results (in case of disturbance)

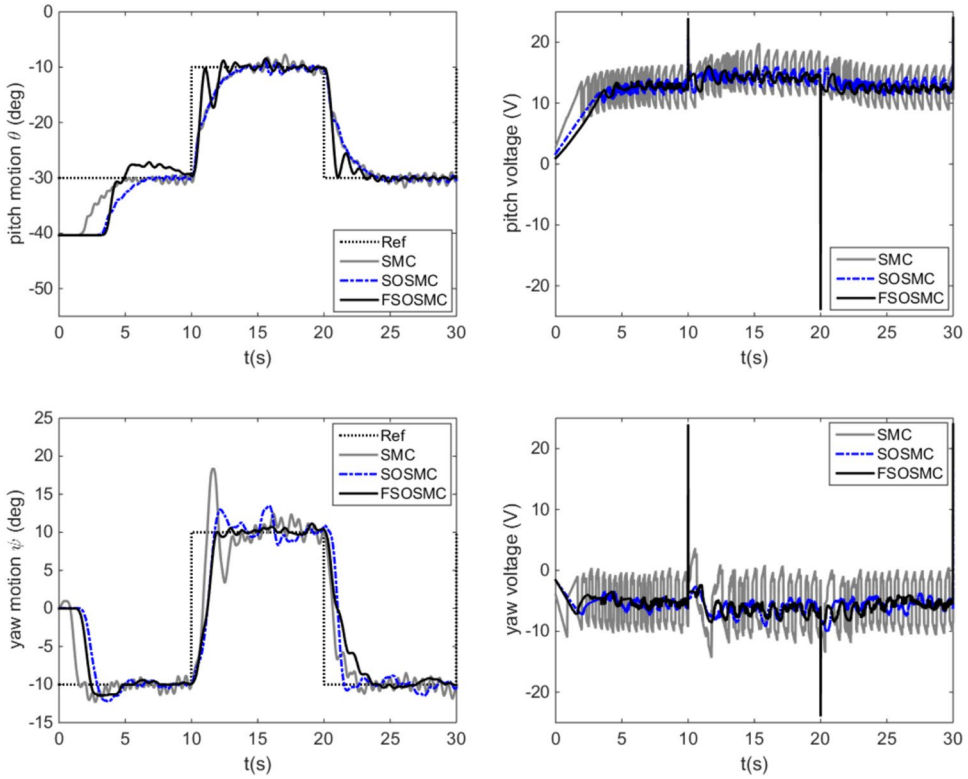

Table 3 Performance indexes (without disturbance)

	θ					ψ				
	SMC	SOSMC	% variation[a]	FSOSMC	% variation[b]	SMC	SOSMC	% variation[a]	FSOSMC	% variation[b]
ITAE	985	973.00	**−1.22**	771	**−21.73**	1050	839.00	**−20.10**	929	**−11.52**
CEI (Nm)	13.3	13.10	**−1.50**	12.6	**−5.26**	6.48	5.94	**−8.33**	5.97	**−7.87**
CI	564	333.00	**−40.96**	332	**−41.13**	563	321	**−42.98**	327	**−41.92**

[a]Variation of performance index (SOSMC vs. SMC)

[b]Variation of performance index (FSOSMC vs. SMC)

Table 4 Performance indexes (in case of disturbance)

	θ					ψ				
	SMC	SOSMC	% variation[a]	FSOSMC	% variation[b]	SMC	SOSMC	% variation[a]	FSOSMC	% variation[b]
ITAE	985	951.00	**−3.45**	738	**−25.08**	863	958.00	**11.01**	908	**5.21**
CEI (Nm)	13.5	12.90	**−4.44**	12.6	**−6.67**	6.77	5.88	**−13.15**	5.86	**−13.44**
CI	581	339.00	**−41.65**	329	**−43.37**	554	328.00	**−40.79**	326	**−41.16**

[a]Variation of performance index (SOSMC vs. SMC)

[b]Variation of performance index (FSOSMC vs. SMC)

is suppressed with the SOSMC and proposed FSOSMC controllers.

To evaluate the success of implemented control algorithms evidently, the performance indexes given in Eqs. (62)–(64) were additionally calculated and given in Tables 3 and 4. It is observed from Table 3 that when there is no external disturbance the ITAE index for the pitch motion is smaller with FSOSMC than the first order SMC and classical SOSMC. For the yaw motion both classical SOSMC and proposed FSOSMC performed better than the SMC whereas classical SOSMC is slightly better than the proposed controller. Additionally, it is worth noting that this success is achieved without increasing the control effort. It really appears that CEI and CI indexes are smaller that is less control effort and chattering is used by both classical SOSMC and proposed FSOSMC when compared with the SMC. Similarly, it was observed from Table 4 that when there is external disturbance the ITAE index for FSOSMC is smaller than the one for classical SOSMC for both pitch and yaw motions. Additionally, it is observed that the designed second order sliding mode controllers utilized less control effort when compared to the first order SMC, and the chattering index of the first order SMC is greater. This reveals that with the proposed FSOSMC the performance is increased without increasing control effort while decreasing chattering.

Conclusion

A novel FSOSMC, in which the sliding surface parameters were tuned by means of a fuzzy logic algorithm, was proposed for the twin rotor system in this study. The aim was to increase the tracking performance of the twin rotor system and to suppress the chattering without increasing the control effort. To demonstrate the performance of the proposed FSOSMC, real-time experiments were conducted on the twin rotor system. When the time responses were investigated it revealed that the fuzzy logic tuning has increased the performance of the FSOSMC without increasing the control effort. Additionally, by using the second order sliding mode based control with super twisting algorithm in FSOSMC, paved the way to suppress chattering. The reduction in chattering increases the applicability of the controller in real time. The performance of the designed controllers was confirmed by the calculated trajectory tracking, control effort and chattering performance indexes based on the experimental results. In conclusion, considering the results obtained in this study reveals that the proposed FSOSMC outperformed the classical SMC and SOSMC since proposed controller provided better performance indexes in most cases. Therefore, proposed FSOSMC may be recommended for the robust and precise control of aerial vehicles in real time.

Appendix 1

Energy Functions for Lagrange's Method

$$K = \frac{1}{2}m_{hel}\left(l^2(\dot{\psi})^2 cos^2(\theta) + l^2(\dot{\theta})^2\right) + \frac{1}{2}I_{pitch}(\dot{\theta})^2 + \frac{1}{2}I_{yaw}(\dot{\psi})^2 \tag{65}$$

$$D = \frac{1}{2}B_{pitch}(\dot{\theta})^2 + \frac{1}{2}B_{yaw}(\dot{\psi})^2 \tag{66}$$

$$P = m_{hel}glsin(\theta) \tag{67}$$

Here K is the total kinetic energy of the system, D is the damping term, and P is the potential energy of the system. The equations of motion for the twin rotor system given in Eqs. (1)–(2) may be obtained by using the following Lagrange's equation:

$$\frac{d}{dt}\left(\frac{\partial K}{\partial \dot{q}_i}\right) - \frac{\partial K}{\partial q_i} + \frac{\partial D}{\partial \dot{q}_i} + \frac{\partial P}{\partial q_i} = Q_i \tag{68}$$

Table 5 The parameters of the twin rotor model

Model parameters	Symbol	Value	Unit
Helicopter helicopter's total moving mass	m_{hel}	1.3872	kg
Distance of mass center along helicopter body from pitch axis	l	0.186	m
Viscous damping for pitch axis	B_{pitch}	0.8	N/V
Viscous damping for yaw axis	B_{yaw}	0.318	N/V
Total mass moment of inertia (pitch axis)	I_{pitch}	0.0384	kgm^2
Total mass moment of inertia (yaw axis)	I_{yaw}	0.0432	kgm^2
θ initial value	$\theta(0)$	−40.3	°
ψ initial value	$\psi(0)$	0	°
Electrical motor parameters			
Thrust force constant of yaw motor	K_{pp}	0.204	Nm/V
Thrust torque constant acting on pitch axis from yaw motor	K_{py}	0.0068	Nm/V
Thrust torque constant acting on yaw axis from pitch motor	K_{yp}	0.0219	Nm/V
Thrust torque constant acting on yaw axis from yaw motor	K_{yy}	0.072	Nm/V
Pitch motor limit voltage	V_{mp}	24	V
Yaw motor limit voltage	V_{my}	24	V

where q_i is the generalized coordinate and Q_i is the generalized force (Table 5).

Appendix 2

First Order Sliding Mode Controller Design

State equations are:

$$\dot{x_1} = x_2 \tag{69}$$

$$\dot{x_2} = f(x_1, x_2) + g(x_1, x_2)\overline{u} + \overline{d} \tag{70}$$

x_1, x_2 are state variables, control input is denoted with $\overline{u}$ and exogenous disturbance is denoted with $\overline{d}$, $\left|\overline{d}\right| \le \Delta$, $\Delta > 0$. Sliding surface is:

$$\sigma = \alpha(x_{1r} - x_1) + (\dot{x}_{1r} - \dot{x_1}) \tag{71}$$

with $\alpha > 0$. Suppose that Lyapunov function and its derivative are

$$V = \frac{1}{2}\sigma^2 \tag{72}$$

$$\dot{V} = \sigma\dot{\sigma} \tag{73}$$

From limit condition of Eq. (73) then

$$\dot{\sigma} = \alpha(\dot{x}_{1r} - \dot{x}_1) + (\ddot{x}_{1r} - \ddot{x}_1) = 0 \tag{74}$$

Utilizing Eqs. (69), (70) and (74), the equivalent control $\overline{u}_{eq}$ is obtained as:

Table 6 Gains of the classical first order SMC

SMC	k_θ	6.37
	k_ψ	3.20

$$\overline{u}_{eq} = g^{-1}(x_1, x_2)\{\alpha(x_{2r} - x_2) + \dot{x}_{2r} - f(x_1, x_2)\} \tag{75}$$

Then entire control input is selected as;

$$\overline{u} = \overline{u}_{eq} + kg^{-1}(x_1, x_2)sign(\sigma) \tag{76}$$

Thus $\dot{V}$ becomes:

$$\begin{aligned}\dot{V} &= \sigma\dot{\sigma} \\ &= \sigma\left\{\alpha(x_{2r} - x_2) + \left(\dot{x}_{2r} - f(x_1, x_2) - g(x_1, x_2)\overline{u} - \overline{d}\right)\right\} \\ &= -k\sigma sign(\sigma) - \sigma\overline{d} \le -|\sigma|(k - \Delta)\end{aligned} \tag{77}$$

If $k > \Delta$ then $\dot{V}$ is negative definite, reaching to the sliding surface is assured.

If a similar estimation as SOSMC in Eq. (33) is used and if the governing yaw and pitch Eqs. (4)–(7) are used, then control rule for the first order SMC for twin rotor becomes

$$\overline{\tau}_\theta = \widehat{\overline{\tau}_{eq\theta}} + k_\theta(m_{hel}l^2 + I_{pitch})sign\{(\alpha_\theta(x_{1r} - x_1) + \dot{x}_{1r} - x_2)\} \tag{78}$$

$$\left(\widehat{\dot{\overline{\tau}}_{eq\theta}}\right) = \varepsilon\left(\overline{\tau}_\theta - \widehat{\overline{\tau}_{eq\theta}}\right) \tag{79}$$

$$\begin{aligned}\overline{\tau}_\psi = \widehat{\overline{\tau}_{eq\psi}} + k_\psi(m_{hel}l^2cos^2(x_1) + I_{yaw}) \\ sign\{(\alpha_\psi(x_{3r} - x_3) + \dot{x}_{3r} - x_4)\}\end{aligned} \tag{80}$$

$$\left(\widehat{\dot{\overline{\tau}}_{eq\psi}}\right) = \varepsilon\left(\overline{\tau}_{\psi} - \widehat{\overline{\tau}_{eq\psi}}\right) \tag{81}$$

Classical Second Order Sliding Mode Controller Design

The control laws for the classical SOSMC are presented below:

$$\overline{\tau_{\theta}} = -\left(m_{hel}l^2 + I_{pitch}\right)\tau_{\theta} \tag{82}$$

$$\begin{aligned}\tau_{\theta} = -k_{1\theta}\left|\alpha_{\theta}\left(x_{1r} - x_1\right) + \dot{x}_{1r} - x_2\right|^{\frac{1}{2}} \\ sign\left(\alpha_{\theta}\left(x_{1r} - x_1\right) + \dot{x}_{1r} - x_2\right) + \upsilon_{\theta}\end{aligned} \tag{83}$$

$$\dot{\upsilon_{\theta}} = -k_{2\theta}\left\{sign\left(\alpha_{\theta}\left(x_{1r} - x_1\right) + \dot{x}_{1r} - x_2\right)\right\} \tag{84}$$

$$\overline{\tau_{\psi}} = -\left(m_{hel}l^2 cos^2(x_1) + I_{yaw}\right)\tau_{\psi} \tag{85}$$

$$\begin{aligned}\tau_{\psi} = -k_{1\psi}\left|\alpha_{\psi}\left(x_{3r} - x_3\right) + \dot{x}_{3r} - x_4\right|^{\frac{1}{2}} \\ sign\left(\alpha_{\psi}\left(x_{3r} - x_3\right) + \dot{x}_{3r} - x_4\right) + \upsilon_{\psi}\end{aligned} \tag{86}$$

$$\dot{\upsilon_{\psi}} = -k_{2\psi}\left\{sign\left(\alpha_{\psi}\left(x_{3r} - x_3\right) + \dot{x}_{3r} - x_4\right)\right\}. \tag{87}$$

Acknowledgements This research received no specific grant from any funding agency in the public, commercial, or not-for-profit sectors.

Funding Open access funding provided by the Scientific and Technological Research Council of Türkiye (TÜBİTAK). The authors did not receive support from any organization for the submitted work.

Data Availability The data are available from the corresponding author on reasonable request.

Declarations

Conflict of interest The authors have no competing interests to declare that are relevant to the content of this article.

Consent to Participate Not applicable.

Consent for Publication The manuscript is approved by all authors for publication.

Ethical Approval Not applicable.

Open Access This article is licensed under a Creative Commons Attribution 4.0 International License, which permits use, sharing, adaptation, distribution and reproduction in any medium or format, as long as you give appropriate credit to the original author(s) and the source, provide a link to the Creative Commons licence, and indicate if changes were made. The images or other third party material in this article are included in the article's Creative Commons licence, unless indicated otherwise in a credit line to the material. If material is not included in the article's Creative Commons licence and your intended use is not permitted by statutory regulation or exceeds the permitted use, you will need to obtain permission directly from the copyright holder. To view a copy of this licence, visit http://creativecommons.org/licenses/by/4.0/.

References

1. Wen P, Lu TW (2008) Decoupling control of a twin rotor MIMO system using robust deadbeat control technique. IET Control Theory Appl 2(11):999–1007
2. Tao CW, Taur JS, Chen YC (2010) Design of a parallel distributed fuzzy LQR controller for the twin rotor multi-input multi-output system. Fuzzy Sets Syst 161(15):2081–2103
3. Taskin Y (2014) Improving pitch and yaw motion control of twin rotor MIMO system. J Vibroeng 16(4):1650–1660
4. Jih-Gau J, Wen-Kai L, Cheng-Yu T (2005) Intelligent control scheme for twin rotor MIMO system. In: IEEE international conference on mechatronics, 2005. ICM'05
5. Aras AC, Kaynak O (2014) Interval type-2 fuzzy neural system based control with recursive fuzzy C-means clustering. Int J Fuzzy Syst 16(3):317–326
6. Hacioglu Y (2015) Multiple-input multiple-output proportional–integral–proportional–derivative type fuzzy logic controller design for a twin rotor system. J Vibroeng 17(6):3104–3110
7. Omar M, Zaidan MA, Tokhi MO (2012) Dynamic modelling and control of a twin-rotor system using adaptive neuro-fuzzy inference system techniques. Proc Inst Mech Eng Part G J Aerosp Eng 226(G7):787–803
8. Juang JG, Liu WK, Lin RW (2011) A hybrid intelligent controller for a twin rotor MIMO system and its hardware implementation. ISA Trans 50(4):609–619
9. Jalalian Khakshour A, Ahmadieh Khanesar M (2016) Model reference fractional order control using type-2 fuzzy neural networks structure: implementation on a 2-DOF helicopter. Neurocomputing 193(Supplement C):268–279
10. Mondal S, Mahanta C (2012) Adaptive second-order sliding mode controller for a twin rotor multi-input-multi-output system. IET Control Theory Appl 6(14):2157–2167
11. Ahmed Q, Bhatti AI, Iqbal S (7th, 2009) Nonlinear robust decoupling control design for twin rotor system. In: Asian control conference, 2009. ASCC 2009
12. Corradini ML, Cristofaro A, Orlando G (2014) Sliding-mode control of discrete-time linear plants with input saturation: application to a twin-rotor system. Int J Control 87(8):1523–1535
13. Ilyas M et al (2016) Control law design for twin rotor MIMO system with nonlinear control strategy. Discret Dyn Nat Soc 2016:10
14. Raghavan R, Thomas S (2017) Practically implementable model predictive controller for a twin rotor multi-input multi-output system. J Control Autom Electr Syst 28(3):358–370
15. Palepogu KR, Mahapatra S (2024) Design of sliding mode control with state varying gains for a benchmark twin rotor MIMO system in horizontal motion. Eur J Control 75:100909. https://doi.org/10.1016/j.ejcon.2023.100909
16. Zeghlache S et al (2022) Twin rotor MIMO system experimental validation of robust adaptive fuzzy control against wind effects. IEEE Syst J 16(1):409–419
17. Utkin VI (1977) Variable structure systems with sliding modes. IEEE Trans Autom Control 22(2):212–222
18. Utkin VIGJ, Shi J (1999) Sliding mode in control in electromechanical systems. Taylor & Francis, London

19. Hacioglu Y, Arslan YZ, Yagiz N (2011) MIMO fuzzy sliding mode controlled dual arm robot in load transportation. J Frankl Inst Eng Appl Math 348(8):1886–1902
20. Nguyen TA (2023) Research on the sliding mode——PID control algorithm tuned by fuzzy method for vehicle active suspension. Forces Mech 11:100206. https://doi.org/10.1016/j.finmec.2023.100206
21. Wijaya AA et al (2024) Adaptive estimation and control of nonlinear suspension systems with natural logarithm sliding mode control. IEEE Access 12:60896–60907. https://doi.org/10.1109/ACCESS.2024.3393970
22. Zhu M et al (2022) Delay-dependent sliding mode variable structure control of vehicle magneto-rheological semi-active suspension. IEEE Access 10:51128–51141
23. Wang C et al (2022) Variable fractional order sliding mode control for seismic vibration suppression of uncertain building structure. J Vib Eng Technol 10(1):299–312
24. Yang H et al (2022) Continuous swept-sine vibration realization combining adaptive sliding mode control and inverse model compensation for electro-hydraulic shake table. J Vib Eng Technol 10(3):1007–1019
25. Zhang L et al (2023) Experiment and simulation research on synchronization control of shaking tables system based on adaptive sliding mode controller. J Vib Eng Technol 11(4):1623–1645
26. Zhang L et al (2024) Fixed-time terminal sliding mode control for uncertain robot manipulators. ISA Trans 144:364–373. https://doi.org/10.1016/j.isatra.2023.10.011
27. Chávez-Vázquez S et al (2023) Trajectory tracking of Stanford robot manipulator by fractional-order sliding mode control. Appl Math Model 120:436–462
28. Laghrouche S, Plestan F, Glumineau A (2007) Higher order sliding mode control based on integral sliding mode. Automatica 43(3):531–537
29. Young KD, Utkin VI, Ozguner U (1999) A control engineer's guide to sliding mode control. IEEE Trans Control Syst Technol 7(3):328–342
30. Edwards C, Spurgeon S (1998) Sliding mode control: theory and applications. Taylor & Francis, London
31. Bartolini G, Ferrara A, Usai E (1998) Chattering avoidance by second-order sliding mode control. IEEE Trans Autom Control 43(2):241–246
32. Levant A (1993) Sliding order and sliding accuracy in sliding mode control. Int J Control 58(6):1247–1263
33. Levant A (2005) Homogeneity approach to high-order sliding mode design. Automatica 41(5):823–830
34. Levant A (2007) Principles of 2-sliding mode design. Automatica 43(4):576–586
35. Bartolini G et al (2000) On multi-input chattering-free second-order sliding mode control. IEEE Trans Autom Control 45(9):1711–1717
36. Fridman L, Levant A (2002) Higher order sliding modes. In: Perruquetti WB, Barbot JP (eds) Sliding mode control in engineering. Marcel Dekker Inc., New York, pp 53–102
37. Danesh M, Jalalaei A, Derakhshan RE (2023) Auto-landing algorithm for quadrotor UAV using super-twisting second-order sliding mode control in the presence of external disturbances. Int J Dyn Control 11(6):2940–2957
38. Rashad R, El-Badawy A, Aboudonia A (2017) Sliding mode disturbance observer-based control of a twin rotor MIMO system. ISA Trans 69:166–174
39. Tapia A, Bernal M, Fridman L (2017) Nonlinear sliding mode control design: an LMI approach. Syst Control Lett 104:38–44
40. Ozer HO, Hacioglu Y, Yagiz N (2018) High order sliding mode control with estimation for vehicle active suspensions. Trans Inst Meas Control 40(5):1457–1470
41. Moreno JA, Osorio M (2008) A Lyapunov approach to second-order sliding mode controllers and observers. In: 47th IEEE conference on decision and control, 2008 (Cdc 2008), pp 2856–2861
42. Konak A, Coit DW, Smith AE (2006) Multi-objective optimization using genetic algorithms: a tutorial. Reliab Eng Syst Saf 91(9):992–1007
43. Yagiz N, Hacioglu Y (2005) Fuzzy sliding modes with moving surface for the robust control of a planar robot. J Vib Control 11(7):903–922
44. Quanser I, Quanser 2 DOF helicopter user and laboratory manuals, Revision 2.3.
45. Ogata K (1997) Modern control engineering. Prentice Hall, London
46. Yagiz N, Hacioglu Y (2009) Robust control of a spatial robot using fuzzy sliding modes. Math Comput Model 49(1–2):114–127
47. Ozer HO (2016) High-order sliding mode control of mechanical systems. In: Institute of graduate studies in science and engineering. Department of Mechanical Engineering, Istanbul University, Istanbul, p 105

Publisher's Note Springer Nature remains neutral with regard to jurisdictional claims in published maps and institutional affiliations.